ISSN 1070-4272, Russian Journal of Applied Chemistry, 2014, Vol. 87, No. 7, pp. 930−936. © Pleiades Publishing, Ltd., 2014.
Original Russian Text © R.D. Apostolova, V.S. Sadovoi, R.P. Peskov, E.M. Shembel', 2014, published in Zhurnal Prikladnoi Khimii, 2014, Vol. 87, No. 7, pp. 928−934.

APPLIED ELECTROCHEMISTRY AND CORROSION PROTECTION OF METALS

Electrolytic Synthesis of FeS_2 for Thin-Layer Lithium Battery

R. D. Apostolova, V. S. Sadovoi, R. P. Peskov, and E. M. Shembel'

Ukrainian State University of Chemical Engineering, pr. Gagarina 8, Dnepropetrovsk, 49005 Ukraine
e-mail: shembel@onil.dp.ua

Received June 17, 2014

Abstract—Purposeful synthesis of iron sulfide FeS_2 films for a lithium battery were purposefully synthesized on a 18N12Kh9T steel cathode from a solution containing Mohr's salt and $Na_2S_2O_3$. Various aspects of synthesis were studied. Thin-film Fe-sulfide synthesis products were tested in a prototype lithium battery and also in a lithium-ion system. The synthesized electrolytic iron sulfide FeS_2 with a marcasite structure is capable of reversible electrochemical transformation with output of 390 mA h g^{-1} in negative electrodes of the lithium-ion system with a $LiMn_2O_4$ counter electrode.

DOI: 10.1134/S1070427214070143

The steadily and rapidly growing miniaturization of electronic technology devices dictates that large-scale production of autonomous miniature power sources is needed. To these belong nano- and micrometer lithium batteries. They find use in microcards, sensors, microbots, medical implants, and other devices. In batteries of this kind, the thickness of film electrodes may reach the micrometer size. The electrodes can be fabricated in different ways. One of these, the electrochemical synthesis, is attractive due to its technical simplicity, ecological safety, high productivity, and low cost. The electrolytically synthesized thin-layer sulfides of transition metals (M = Fe, Co, Ni) have been successfully tested in prototype lithium batteries [1]. These sulfides have been produced from M(II) sulfate solutions in the presence of $S_2O_3^{2-}$. The synthesis products are the sulfides MS_x. Depending on the synthesis conditions, a number of stoichiometric sulfides with deficiency (MS_{1-x}) or excess (MS_{1+x}) of sulfur can be obtained. It seems that the most promising among these electrolytic sulfides are iron sulfides FeS_x owing to their high theoretical specific capacity and low toxicity and cost. The theoretical specific capacity of the sulfide FeS_2 is as high as 890 mA h g^{-1}. However, the electrolytes used to synthesize Fe sulfides are less stable in electrolysis and storage than those for deposition of cobalt and nickel sulfides. It has been shown that the stability of a Fe^{2+}-containing electrolyte can be improved by partial replacement of Fe^{2+} with Co^{2+} or Ni^{2+}, with the subsequent formation of electrolytic bimetal sulfides with higher energy capacity [2].

Electrolytic mono- and bimetal sulfides have their own advantages and disadvantages determined by the discharge capacity, efficiency of multiple conversion in the redox reaction with lithium, ecological safety, cost, and stability of the electrolyte for synthesis of a sulfide [1–5].

A number of studies have been concerned with the deposition of Fe sulfides onto Ti, Au, and Pt [6, 7]. Of interest for lithium batteries are thin-layer sulfide deposits on stainless steel. This is so because corrosion studies of construction materials for lithium batteries (LBs) have revealed the advantage of stainless steel [8, 9], which is widely used in LBs.

It has been impossible to quantitatively produce FeS_2, the most energy-rich among iron sulfides, by electrolysis from a solution containing $FeSO_4$ and $S_2O_3^{2-}$. Recently, orthorhombic sulfide FeS_2 intended for determining and activating the reduction of H_2O_2 has been synthesized on a substrate of tin oxide doped with indium in a solution of Mohr's salt in the presence of $Na_2S_2O_3$.

In the present study, we performed an electrochemical synthesis in order to produce FeS_2 for a lithium battery from a solution containing Mohr's salt and $Na_2S_2O_3$, studied aspects of synthesis of iron sulfides on stainless

steel, and tested Fe sulfide synthesis products in a prototype lithium battery and also in a lithium-ion system.

EXPERIMENTAL

Iron sulfides were deposited onto a 1 × 1 cm 18N12Kh9T stainless steel cathode in the form of a plate or grid in solutions containing (M): $Na_2S_2O_3 \cdot 5H_2O$ 1×10^{-2}–1×10^{-3}, $FeSO_4$ $(NH_4)_2SO_4 \cdot 6H_2O$ 1×10^{-2}–1×10^{-3}, at pH 4.7–5.2. Reagents of analytically pure grade were used without additional purification. The electrolysis was performed in a 200-cm^3 glass vessel at 295–298 K, with the solution agitated with a mechanical rabble at a rate of 180 rpm. A technical-grade VT titanium plate served as the counter electrode; $S_{cathode} : S_{anode} = 1 : 10$.

Cyclic voltammograms (VAs) were obtained in the working deposition solution and in solutions of its separate components at potentials in the range from –1.1 to 0 V relative to the Ag/AgCl reference electrode in order to determine the positions of the redox peaks in the systems under study. Polarization curves were obtained in the deposition solution of a sulfide material by recording the electrode potential 30 s after a stepwise interruption of the current. The synthesis products were quantitatively deposited potentiostatically at the potentials of VA current peaks, with the phase composition of the deposit determined using a DRON-2 diffractometer with CoK_α radiation. The surface morphology of the deposits was determined with an MBI-6 optical microscope. The electrochemical characteristics of the sulfide compounds in the redox reaction with lithium were studied in an isolated three-electrode cell with a lithium counter electrode and Li/Li^+ reference electrode and also in a prototype disk battery of 2325 configuration with an electrolyte composed of ethylene carbonate (EC, Merck), dimethyl carbonate (DMC, Merck), and 1 M $LiClO_4$ (Iodobrom) on a testing stand with a software package. The cyclic VAs were recorded with a VoltaLab analytical radiometer.

RESULTS AND DISCUSSION

To analyze the deposition of Fe sulfides, we obtained cyclic VAs in solutions containing $S_2O_3^{2-}$, $FeSO_4$ $(NH_4)_2SO_4$ and in the deposition electrolytes.

The VA recorded in a solution of 1×10^{-2} M of $S_2O_3^{2-}$ in a scheme with an open-circuit potential (OCP = –0.36 V) → (–1.30 V) → (+0.50 V) → (–0.36 V) shows two current peaks in the cathodic region near –0.80 V and in the anodic region near 0.00–0.15 V (Fig. 1a). Previously it has been found that varying the $S_2O_3^{2-}$ concentration within the range from 7.5×10^{-3} to 7.5×10^{-2} M little affects the reduction current, with a tendency toward its slight decrease upon an increase in the concentration [11]. The nature of the reduction current peak is associated with the reaction

$$S + 2H^+ + 2e \rightleftarrows H_2S_{(aq)}. \quad (1)$$

Colloidal sulfur is formed in the acid medium of $S_2O_3^{2-}$ in accordance with the reactions

$$S_2O_3^{2-} + H^+ \rightleftarrows S + HSO_2^{3-}, \quad (2)$$

$$2H_2S_{(aq)} + HSO_{3(aq)}^- + H^+ \rightleftarrows 3H_2O + 3S. \quad (3)$$

The anodic current peak at the potentials of 0.00–0.15 V is accounted for by the oxidation of the substrate and $S_2O_3^{2-}$ ions.

The intensity of the electrode processes and their nature in the system depend on the concentration of Mohr's salt and the potential sweep rate. The reduction current starts to grow at potentials of –0.90 to –1.00 V and reaches a maximum at –1.10 V, with deposition of Fe occurring. The height of the deposition current grows with increasing Fe^{2+} concentration. In the opposite oxidation process, iron is dissolved at the maximum rate at a potential of –0.45 to –0.57 V. As the Fe^{2+} concentration is raised, the dissolution current grows. The intersection of the curves in the cathodic region is an indication of the nucleation process. Kinetic limitations to the electrode process, depending on the potential sweep rate, are indicated by changes in the height and position of current peaks.

The anodic current peak near 0 V is similar to that observed in the VA recorded in a solution of $S_2O_3^{2-}$ (Fig. 1a) and is attributed by the authors to oxidation processes involving the substrate.

The characteristics of the electrode process at a potential sweep rate of 10 mV s^{-1} in the range OCP → –1.1 V → 0.3 V in the first cycle differ from those in the subsequent cycles (Fig. 2). The reduction begins near the potential of –0.90 V and reaches its peak value near –1.0 V. The profiles of the VA curves in the course of reduction on a "clean" substrate without a sulfide coating are not repeated from one cycle to another. There may be a single reduction peak in the first cycle (Fig. 2, curve *1*); small-amplitude reduction current peaks appear in the second cycle at potentials of –0.86 and –0.95 V (Fig. 2,

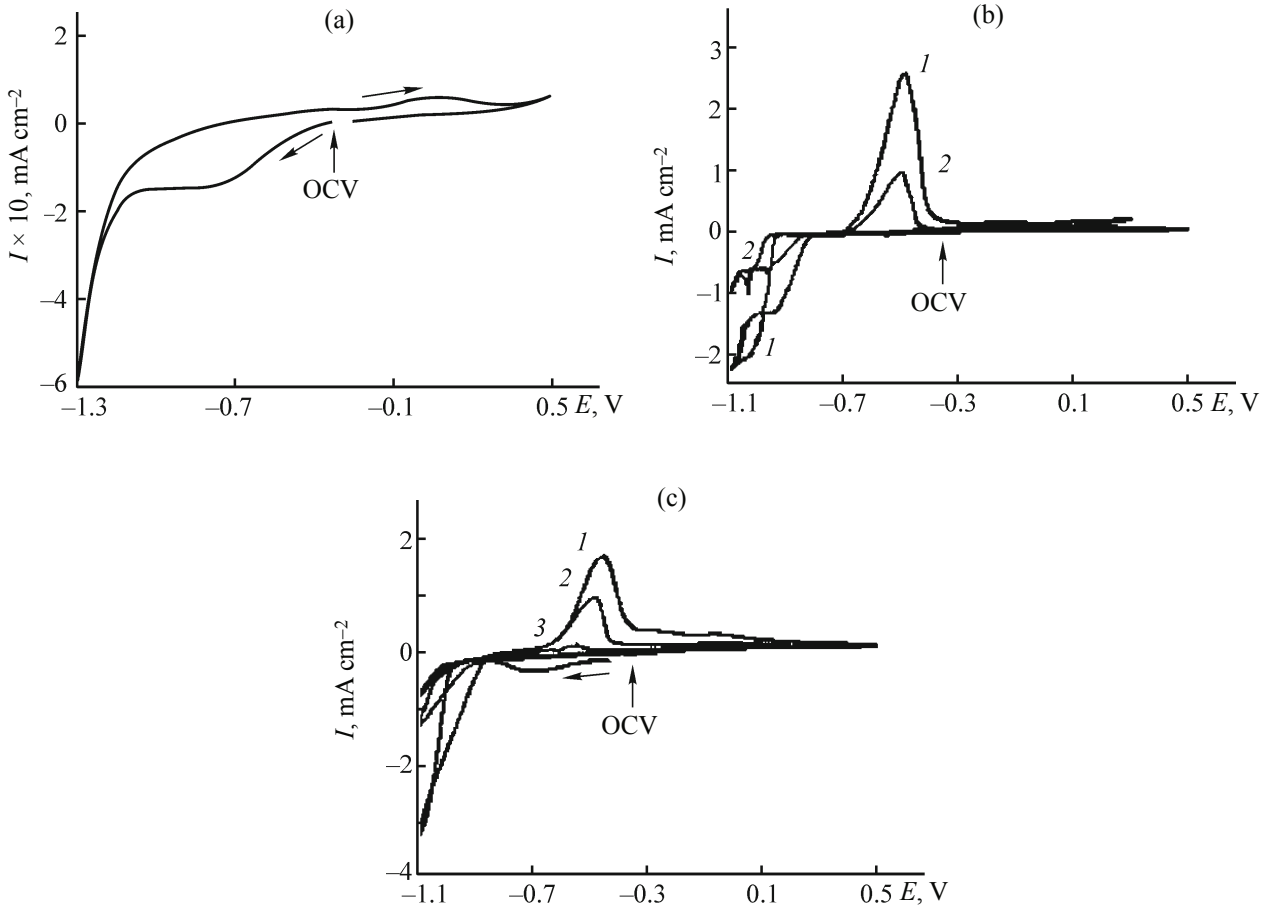

Fig. 1. Cyclic voltammograms for the systems (a) 18N12Kh9T–$S_2O_3^{2-}$ and (b, c) 18N12Kh9T–$FeSO_4$ $(NH_4)_2SO_4$. (*I*) Current and (*E*) potential; the same for Figs. 2–4. Potential sweep rate $v \times 10^4$ (V s^{-1}): (a, c) 10^2 and (b) 5. Concentration of the $FeSO_4(NH_4)_2SO_4$ salt (M): (*1*) 0.010, (*2*) 0.005, and (*3*) 0.001.

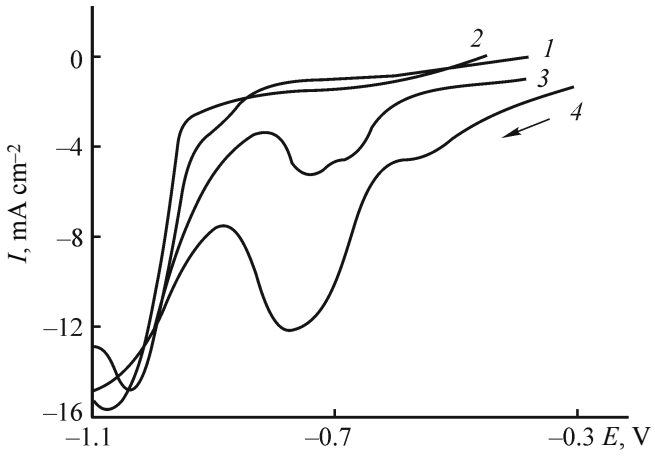

Fig. 2. Voltammogram of the cathodic reduction of the solution of $FeSO_4(NH_4)_2SO_4$–$S_2O_3^{2-}$ in (*1*) first, (*2*) second, (*3*) third, and (*4*) eighth cycles. Potential sweep rate $v = 10^2$ V s^{-1}.

curve *2*); two current bursts are observed near –0.70 V in the third cycle (Fig. 2, curve *3*); in the eighth cycle these become more pronounced and are shifted to potentials of –0.78 and –0.58 V (Fig. 2, curve *4*). There also occurs transformation of the entire VA profile. The VA profile becomes more stable in cycling as the substrate coverage by synthesis products grows.

In the course of oxidation, a change in the slope of the anodic curve, i.e., a change of oxidation stages, are observed up to the final potential of 0.3 V. Anodic current peaks were observed at potential near –0.56...–0.65, –0.10, and 0.00 V (Fig. 3). The VAs obtained in the deposition solution (Fig. 3) show that the electrode process depends on the potential sweep rate and the Mohr's salt concentration.

In the concentration range under study of $S_2O_3^{2-}$ ions in the deposition solution, their reduction can occur without any kinetic hindrance, as shown before for the

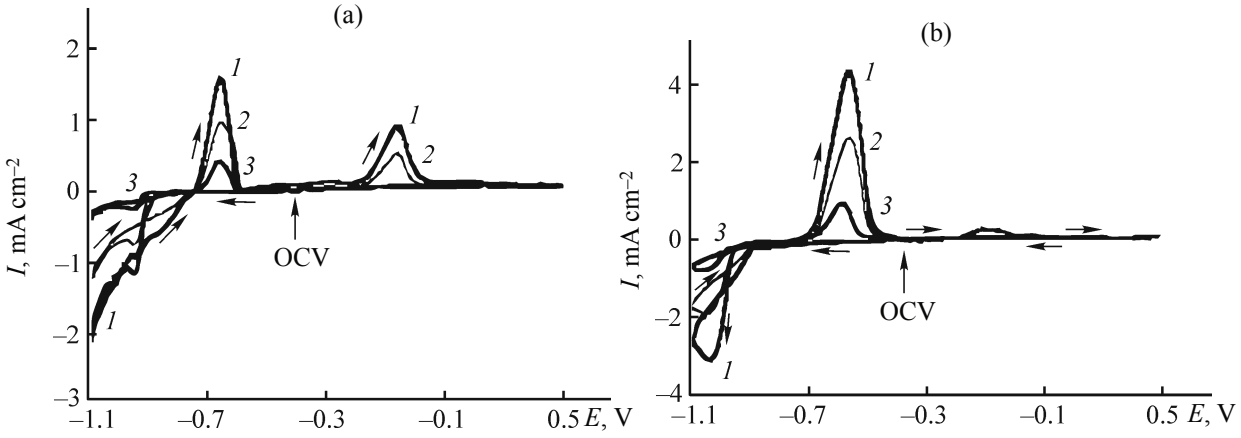

Fig. 3. Cyclic voltammograms of the system 18N12Kh9T–$FeSO_4(NH_4)_2SO_4$–$S_2O_3^{2-}$. Potential sweep rate $v \times 10^4$ (V s^{-1}) (a) 5 and (b) 100. Concentration of the $FeSO_4(NH_4)_2SO_4$ salt (M): (*1*) 0.010, (*2*) 0.005, and (*3*) 0.001.

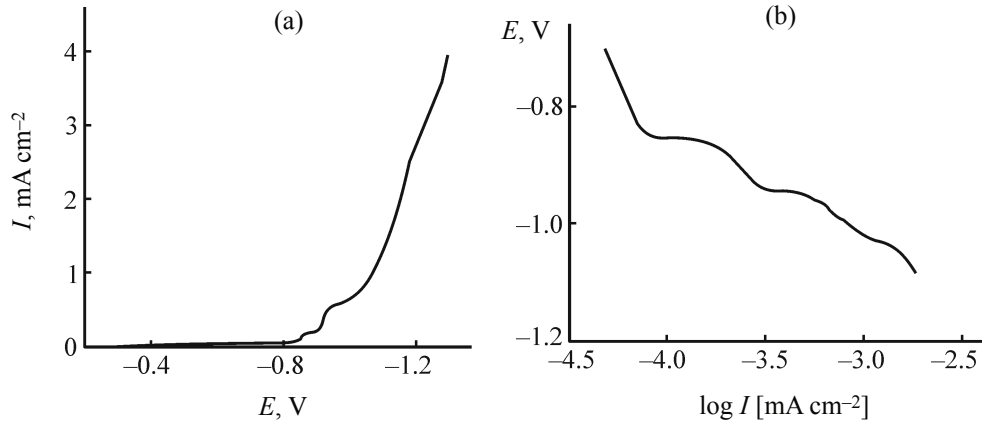

Fig. 4. Cathodic polarization curves in the coordinates (a) *E*–*I* and (b) *E*–log *I*, obtained in a solution containing (M): $0.01FeSO_4(NH_4)_2SO_4 \cdot 6H_2O$ and $0.01Na_2S_2O_3 \cdot 5H_2O$.

pure $S_2O_3^{2-}$ solution. By contrast, the electrochemical conversion in the $Fe^{2+} \leftrightarrow Fe$ process experiences a kinetic hindrance that may be due to, among other things, the delivery of Fe^{2+} ions to the cathode. In this case, transport processes involving Fe^{2+} ions may be a reason for the kinetic hindrance to the electrode process in the system 18N12Kh9T–$FeSO_4(NH_4)_2SO_4$–$S_2O_3^{2-}$. Another possible reason the slower rate of the chemical reaction in which iron sulfide is formed, with Fe^{2+} and S^{2-} involved.

The transformation of VAs in cycling in the deposition electrolyte is accounted for by the influence of the substrate materials on the electrode process. At the beginning of cycling, the electrode reactions occur on a clean stainless steel substrate. As deposit is formed, it is covered by the synthesis products. The key role in the formation of sulfide compounds is played by the reaction

$$S_2O_3^{2-} + 2e \rightleftarrows SO_3^{2-} + S^{2-}, \quad (4)$$

which depends on the substrate material. The difference in the reduction of $S_2O_3^{2-}$ ions on stainless steel and on a sulfide coating is due to that between the electrochemical activities of $S_2O_3^{2-}$ ions on these materials and to their different absorption capacities for the reduction products being formed, sulfide and sulfite ions. As a criterion for the possibility and high intensity of the $S_2O_3^{2-}$ reduction processes can serve the zero-charge potential of the surface of the electrode material [12]. It has been shown previously that, in potentiodynamic deposition of iron sulfides from a solution of $FeSO_4 \cdot 6H_2O$ in the presence of $S_2O_3^{2-}$ ions, the VA profiles measured on stainless steel and titanium substrates depend on the substrate material [11].

The electrode process in syntheses of electrolytic iron sulfides was also analyzed using the polarization curves.

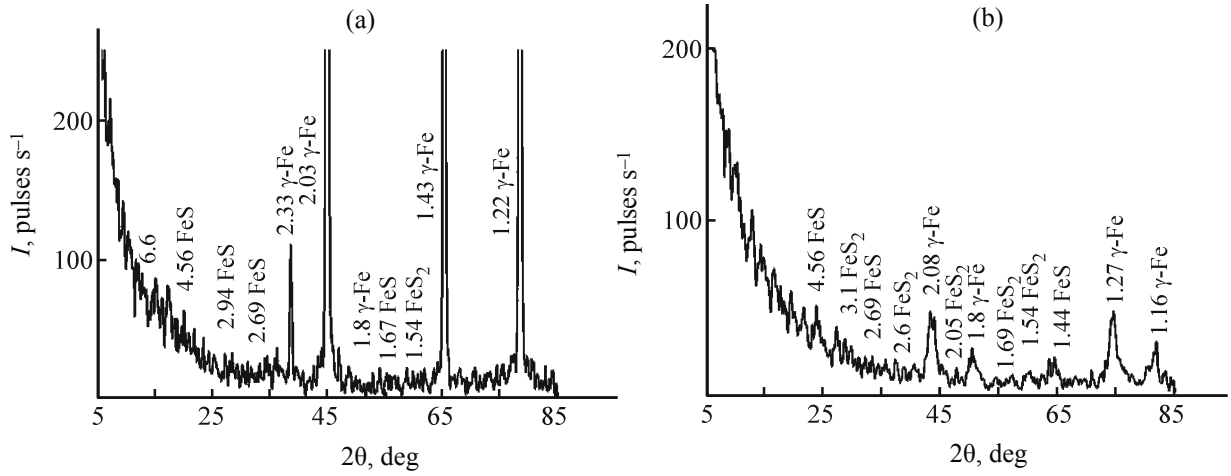

Fig. 5. X-ray diffraction patterns of deposits obtained at potentials of (a) –0.86 and (b) –0.95 V. (*I*) Reflection intensity and (2θ) Bragg angle. γ-Fe are reflections from the substrate.

The polarization curves plotted in the coordinates *I*–*E* and *E*–log *I* in Fig. 4 demonstrate that three main stage transitions successively occur in deposition of iron sulfides at potentials in the range –0.35 to –1.20 V. To the horizontal portions of the polarization curves at potentials of –0.86, –0.95, and 1.00 × –1.10 V correspond separate-phase formation stages.

The phase composition of the deposit was determined by X-ray phase analysis.

The structure and composition of the electrolytic iron sulfides are determined by the conditions of the cathodic reduction of the electrolyte and by the nature of a metallic substrate [1, 5]. The phase compositions of the iron sulfides synthesized at VA current peak potentials of –0.86 and –0.95 V in the present study are different.

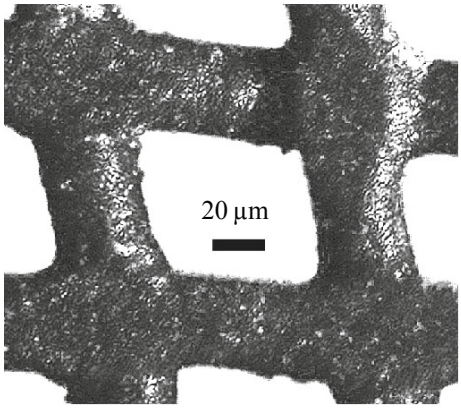

Fig. 6. Optical microscopic image of the surface of the FeS_2 deposit on a stainless steel grid. Magnification ×350.

The sulfide FeS with a cubic structure was identified in the finely crystalline deposit synthesized at a potential of –0.86 V (JCPDS ID 23-1121) (Fig. 5a). The products of synthesis at a potential of –0.95 V are the sulfide FeS_2 with a marcasite structure (JCPDS ID 37–0475) (Figs. 5 and 6) and an admixture of FeS with cubic structure. The size of FeS_2 crystallites was determined using the Debye–Scherrer formula to be 35.5 nm.

Attempts to quantitatively obtain a FeS_2 deposit with a satisfactory adhesion to the metallic support encounter a difficulty of retaining the deposit on a substrate in washing with water. This occurs because finely dispersed iron is deposited together with iron sulfide in the course of its synthesis. The chemical activity of finely dispersed iron is very high. It reacts with water to rapidly give a brown-yellow iron hydroxide, whose flaky particles are detached from the metallic substrate. The swelling of iron hydroxide in the deposit impairs its adhesion capacity.

Remnants of flaky particles of the brown-yellow iron hydroxide are seen on the surface of the black sulfide deposit FeS_2 obtained in the present study.

The optical microscopic images of the surface of electrolytic sulfide FeS_2 films show thread-like formations. Separate particles are indistinguishable in these formations (Fig. 6), which are significantly smaller in size than iron sulfide compounds deposited from the electrolyte containing $FeSO_4 \cdot 6H_2O$–$Na_2S_2O_3 \cdot 5H_2O$ [1, 4]. These latter include spheroidal agglomerates with sizes of 3–5 μm, composed of nanometer-size particles (200–400 nm).

Possible reactions in the cathodic and anodic processes

Potential of the cathodic current peak, V	Reaction	E_0, V
	Possible cathodic reactions	
–0.5 × –0.8	$S_2O_3^{2-} + 2e \rightleftarrows SO_3^{2-} + S^{2-}$ (4) $FeOOH + S + 3H^+ + 3e \rightleftarrows FeS + 2H_2O$ (5) $S + 2H^+ + 2e \rightleftarrows H_2S_{(aq)}$ (6) $Fe^{2+} + S + 2e \rightleftarrows FeS$ (7) $Fe^{2+} + S_2O_3^{2-} + 6H^+ + 6e \rightleftarrows FeS_2 + 3H_2O$ (8) $S_2O_3^{2-} + 6H^+ + 4e \rightleftarrows 2S + 3H_2O$ (9) $S + 2e \rightleftarrows S^{2-}$ (10)	
–0.8 × –1.1	$Fe^{2+} + 2e \rightleftarrows Fe$ (11) $2H_2O + 2e \rightleftarrows H_2 + 2OH^-$ (12)	
	Possible anodic reactions	
–0.5 × –0.6	$Fe \rightleftarrows Fe^{2+} + 2e$ (13) $H_2S \rightleftarrows S + 2H^+ + 2e$ (14) $FeS \rightleftarrows Fe^{2+} + S + 2e$ (15) $Fe^{2+} + 2H_2O \rightleftarrows FeOOH + 3H^+ + e$ (16) $2S_2O_3^{2-} \rightleftarrows S_4O_6^{2-} + 2e$ (17) $Fe^{2+} \rightleftarrows Fe^{3+} + e$ (18)	–0.441 0.080 0.771

Based on the results obtained, we assume that separate stages of the cathodic process may correspond to reactions with current peak potentials listed in the table.

According to [10], FeS_2 is synthesized at the anode via formation by reaction (5) of an intermediate product that subsequently dissociates to give FeS_2:

$$m\mathrm{Fe}^{2+} + n\mathrm{S_4O_6^{2-}} + me + x\mathrm{H_2O} \rightleftarrows [\mathrm{Fe}_m(\mathrm{S_4O_6})_n\cdot(\mathrm{H_2O})_x]^{-(2n-m)},\ E_0 = 0.05\ \mathrm{V}. \quad (5)$$

The multitude of the possible electrode reactions means that it is difficult to obtain an electrolytic single-phase sulfide compound on stainless steel in the electrolyte under study.

In the present study, we examined the deposition of electrolytic sulfides onto the cathode. We believe that sulfide ions formed in reaction (4) are adsorbed on the cathode surface and, entering into a chemical reaction with Fe^{2+} ions from the near-cathode layer, form sulfide compounds of iron.

Among the iron sulfides synthesized in the study, FeS_2 marcasite produced at a potential of –0.95 V has the best discharge characteristics. The discharge capacity of the lithium battery based on this sulfide is more than 900 mA h g^{-1} in the first cycle, and the reversible capacity is 620–800 mA h g^{-1} (Fig. 7).

On being tested in the prototype lithium battery, the electrolytic sulfide FeS_2 was subjected to successful tests in the negative electrode of a lithium-ion system (Fig. 8), with $LiMn_2O_4$ spinel from Merck used in the positive electrode. It charge-discharge characteristics in a prototype lithium battery are shown in Fig. 8.

It was shown that the electrode materials being tested in the lithium-ion system are compatible and the system is capable of multiple electrochemical conversions. The

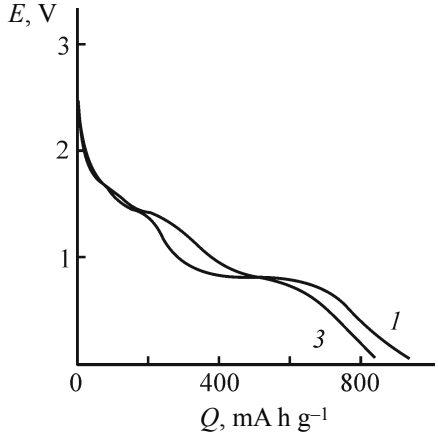

Fig. 7. Discharge curves of the electrolytic FeS_2 in a lithium battery in (*1*) first and (*2*) third cycles. I_{dis} = 0.05 mA cm^{-2}, FeS_2 mass is 0.96 mg cm^{-2}. (*E*) Potential and (*Q*) capacity; the same for Fig. 8.

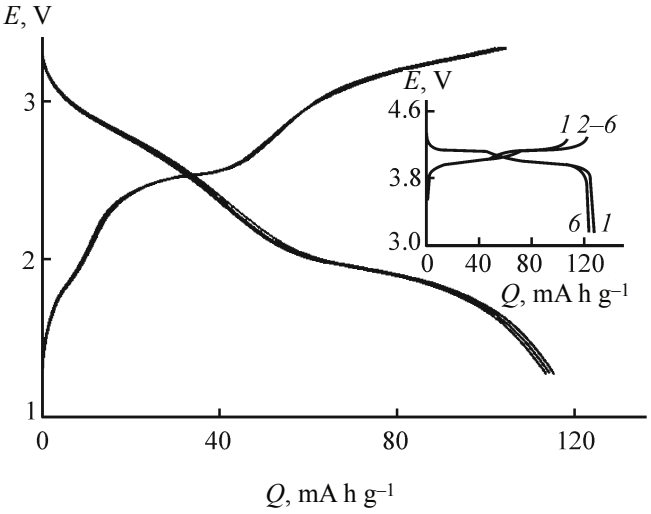

Fig. 8. Charge-discharge curves for the system $LiMn_2O_4$–EC, DMC, 1 M–$LiClO_4$–FeS_2 in cycles from second to sixth. Mass (mg cm^{-2}): $LiMn_2O_4$ spinel 4.4 and FeS_2 0.96. The inset shows charge- discharge curves for the system $LiMn_2O_4$–EC, DMC, 1 M–$LiClO_4$–Li in cycles from second to sixth. $I_{dis} = I_{ch} =$ 0.05 mA cm^{-2}. The capacity Q is calculated per gram of spinel.

average discharge voltage of the lithium-ion system is 2 V (Fig. 8).

The discharge capacity of the electrolytic sulfide FeS_2 in the sixth cycle this system reaches a value of 390 mA h g^{-1}.

CONCLUSIONS

(1) The conditions were determined in which iron disulfide FeS_2 is obtained in the form of thin films with a mass of 0.4–1.5 mg cm^{-2} on a stainless steel cathode from an aqueous solution of Mohr's salt in the presence of sodium thiosulfate. The structure of the resulting iron disulfide corresponds to the orthorhombic structure of marcasite. It is shown that this disulfide can be used in a thin-layer lithium-ion system as the active material in the negative electrode. The discharge capacity of the electrolytic FeS_2 marcasite exceeds the specific theoretical capacity of graphite (372 mA h g^{-1}) used in commercial lithium-ion systems.

(2) A potentiodynamic study demonstrated that the deposition of FeS_2 onto the cathode occurs simultaneously with the formation of iron. Finely dispersed iron has an increased chemical activity and its interaction with water in washing of the deposit easily yields iron hydroxide. The swelling of the admixture of iron hydroxide impairs the adhesion of the sulfide deposit to the metallic base. It is known that the electrochemical characteristics of FeS_2 with a pyrite structure are advantageous over those of its analog with a marcasite structure in the redox reaction with lithium.

REFERENCES

1. Nagirnyi, V.M., Apostolova, R.D., and Shembel', E.M., *Sintez i elektrokhimicheskie kharakteristiki elektroliticheskikh metallo-oksidnykh i metallo-sul'fidnykh soedinenii dlya litievykh akkumulyatorov* (Synthesis and Electrochemical Characteristics of Metal-Oxide and Metal-Sulfide Compounds for Lithium Batteries), Dnepropetrovsk: GVUZ UDKhTU, 2008.
2. Apostolova, R.D., Kolomoets, O.V., Nagirnyi, V.M., and Shembel', E.M., *Vopr. Khim. Khim. Tekhnol*., 2010, no. 1, pp. 161-163.
3. Apostolova, R.D., Tysyachnyi, V.P., and Shembel', E.M., *Russ. J. Electrochem*., 2010, vol. 46, no. 1, pp. 100–106.
4. Shembel', E.M., Apostolova, R.D., Nagirnyi, V.M., et al., *Russ. J. Electrochem*., 2004, vol. 40, no. 7, pp. 736–742.
5. Apostolova, R.D., Nagirnii, V.M., Kolomoets', O.V., et al., *Vopr. Khim. Khim. Tekhnol*., 2011, no. 11, pp. 147–151.
6. Yufit, V., Freedman, K., Nathan, M., et al., *Electrochim. Acta*, 2004, pp. 417–420.
7. Gomes A., da Silva Pereira, M.I., Mendonza, M.H., et al., *Electrochim. Acta*, 2004, vol. 49, pp. 2155–2165.
8. Apostolova, R.D., Shembel', E.M., and Strizhko, A.S., *Zh. Prikl. Khim*., 1989, vol. 62, no. 10, pp. 2232–2236.
9. Apostolova, R.D., Shembel', E.M., and Petrunin, G.P., *Zh. Prikl. Khim*., 1990, vol. 63, no. 9, pp. 2069–2073.
10. Biswajit Chakraborty, Bibhutibhushan Show, Sumanta Jana, et al., *Electrochim. Acta*, 2013, vol. 94, p. 7–15.
11. Apostolova, R.D., Kolomoets, O.V., and Shembel', E.M., *Vopr. Khim. Khim. Tekhnol*., 2011, no. 2, pp. 147–151.
12. Gur'yanova, I.A., Omel'chuk, A.A., and Shvab, N.A., *Visnik Kharkiv Nats. Univ*., 2005, vol. 648, no. 12, pp. 264–267.